

# Effect of Substrate Roughness on Splating Behavior of HVOF Sprayed Polymer Particles: Modeling and Experiments

*M. Ivosevic, V. Gupta, R. A. Cairncross, T. E. Twardowski, R. Knight,  
Drexel University, Philadelphia, Pennsylvania, USA*

*J. A. Baldoni  
Duke University, North Carolina, USA*

## Abstract

A three-dimensional model of particle impact and deformation on rough surfaces has been developed for HVOF sprayed polymer particles. Fluid flow and particle deformation was predicted by the Volume of Fluid (VoF) method using Flow-3D<sup>®</sup> software. The effect of roughness on the mechanics of splatting and final splat shapes was explored through the use of several prototypical rough surfaces, e.g. steps and grooves. In addition, a numerical representation of a more realistic rough surface, generated by optical interferometry of an actual grit blasted steel surface, was also incorporated into the model. Predicted splat shapes were compared with SEM images of Nylon 11 splats deposited onto grit blasted steel substrates. Rough substrates led to the generation of fingers and other asymmetric three-dimensional instabilities that are seldom observed in simulations of splatting on smooth substrates.

## Introduction

It is well understood and commonly accepted that substrate roughness enhances bonding and adhesion of thermally sprayed coatings [1]. Before spraying, substrate surfaces are typically roughened by grit blasting with 50 – 300  $\mu\text{m}$  angular ceramic particles such as alumina or SiC. The morphology of the initial splats deposited onto a substrate surface play an important role in the integrity of the coating/substrate interface and the resulting coating's adhesive strength.

The impact and deformation of thermally sprayed droplets on a rigid, irregular surface are characterized by complex large-scale three-dimensional deformation of droplet surfaces. In cases where “splashing” of impacting droplets occurs, the creation of new surfaces during fingering and/or the generation of satellite particles and breakup is typically not axisymmetric, which would require a three-dimensional model for realistic splat predictions. This creates number of

numerical challenges for the development of an accurate three dimensional splatting model. Fauchais et al. [2] reported that the majority (~98 %) of published papers concerning splat formation processes, describe normal droplet impact onto a smooth surface. Less than 2% of published work relates to non-normal particle impacts on smooth surfaces and only ~0.1 % relates to rough substrates. Several authors [3, 4] have studied the interactions of a droplet with non-smooth surfaces using two-dimensional models or three-dimensional impacts on surfaces with parallel groves [5], however, the main disadvantage of this approach is the inability to study the non-axisymmetric aspects of splatting on a rough surface. Recently, Raessi et al. [6] expanded a previously developed VoF model [7] for droplet splatting on flat substrate to droplet interaction with a prototypical rough surface. The surface roughness was approximated by regularly ordered square blocks. Feng et al. [8] used a three-dimensional Lagrangian finite-element model where the surface roughness was approximated by a frictional condition on a flat surface. Although this approach can be very accurate with respect to small scale viscous and axisymmetric free surface flows, droplet splashing involving the creation of new surfaces during fingering and/or generation of satellites and breakups are not amenable to boundary-fitted techniques. Moreover, the average surface roughness ( $R_a$ ) of a grit blasted surface used for thermal spray is typically ~ 5 – 30 % (~ 2 - 15  $\mu\text{m}$ ) relative to a mean droplet size of 50  $\mu\text{m}$  which may be too large to be approximated by simple frictional flow on a flat surface.

The goal of this work is to develop a model of HVOF sprayed polymer particles impacting onto an arbitrary rough substrate. A particle splatting model on non-smooth surfaces would provide a better understanding of how the geometrical irregularities of a surface affect the splatting behavior and final splat morphology.

## Background

Forced convection from an HVOF jet to a micron sized feedstock particle is characterized by a high convective heat transfer coefficient ( $h \sim 5000 - 17,000 \text{ W}/(\text{m}^2\text{K})$ ). This results in a rapid increase in particle surface temperature, however, the high internal thermal resistance (high Bi number) of polymer particles prevents the interior of the particle from being heated at the same rate. As a result, larger (e.g.  $90 \mu\text{m}$  diameter) Nylon 11 particles develop a steep temperature gradient between the core and surface prior to impact on a substrate (Figure 1) [9, 10, 11].

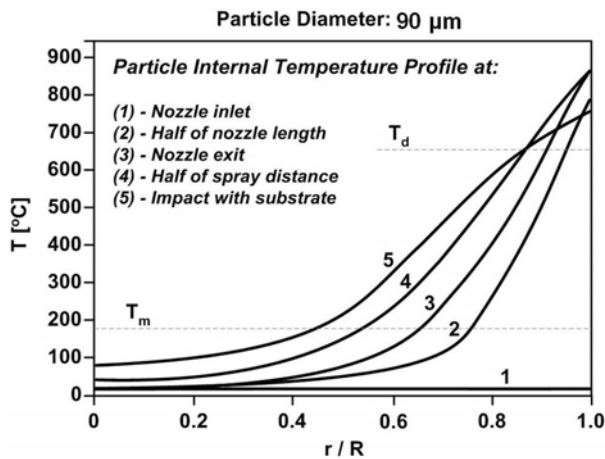


Figure 1: Temperature of a  $90 \mu\text{m}$  diameter Nylon 11 particle with respect to normalized particle radius ( $r/R$ ) [10].

It was also previously reported [10] that HVOF sprayed polymer particles with steep internal temperature gradients spread into a characteristic “fried-egg” shape with a large, nearly-hemispherical, core in the center of a thin disk (Figure 2). This shape indicated the existence of a large radial difference between the flow properties of the low temperature, high viscosity core and the high temperature, low viscosity surface. The predicted shapes of deformed particles (Figure 2a) exhibited good qualitative agreement with experimentally observed splats deposited onto a glass slide (Figure 2b). The velocity field vectors shown in the right-hand side of the droplet (Figure 2a) indicated that the characteristic “fried-egg” splat shape was formed as the low viscosity “skin” flowed around a high viscosity core.

The HVOF spray parameters used during the experiments reported in this work represent typical HVOF spray parameters that can be used to deposit Nylon 11. A numerical model developed around the experimental baseline parameters, however, can be used to better understand the flow behavior of individual splats and assist in process optimization for increased deposition efficiency.

The previously developed approach for the spreading of the HVOF sprayed Nylon 11 particles on a flat substrate [10, 12] has been used here to further study the interaction of individual splats with an arbitrary rough substrate. Preliminary results of this study are presented below.

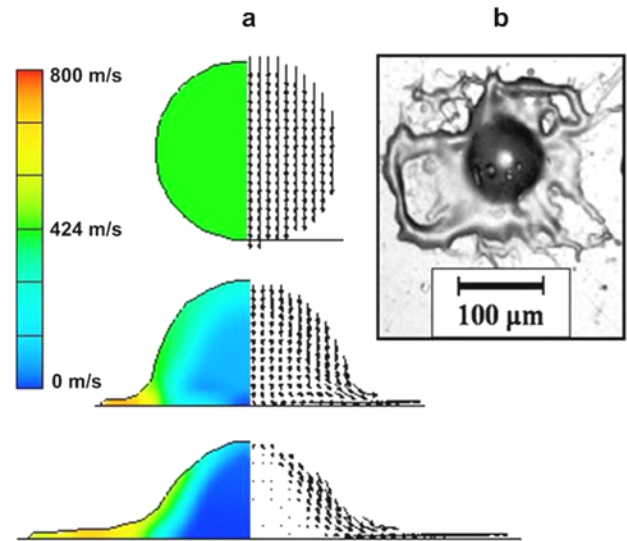


Figure 2: (a) Velocity field within a spreading  $90 \mu\text{m}$  diameter particle; (Left): velocity magnitude, (Right): velocity vectors, (b) example Nylon 11 splat deposited via swipe test onto a room temperature glass slide.

## Mathematical Modeling

Mathematical models have been developed to predict the particle transport and deformation on impact with a flat substrate during the HVOF combustion spraying of polymeric materials. The models of particle acceleration and heating in an HVOF jet are fully coupled and simultaneously integrated within the same FORTRAN code in order to predict particle velocity and temperature profiles at impact. A Volume-of-Fluid [13] computational fluid mechanics package, Flow-3D<sup>®</sup>, was used to predict splat shapes using results from the acceleration and heating models as initial conditions. A 2D slice of the computational domain including a fixed grid and a schematic representation of the initial and boundary conditions used here is shown in Figure 3. Further details of the mathematical models used to predict the particle transport and deformation on impact and to predict splat shapes presented have been reported elsewhere [10, 12].

As described earlier, most of the polymer particles under HVOF conditions have higher temperatures at the surface than at the core. Consequently, during particle impact and spreading the local Reynolds number varies across the droplet owing to the temperature-dependent viscosity distribution. Moreover, when the particle begins deforming, the particle

viscosity is also altered, based on the local fluid velocity (i.e. the local shear rate). Polymer viscosity during droplet spreading is therefore a function of both the temperature and shear rate. The shear rate and temperature-dependent viscosity of Nylon 11 was predicted using a Carreau model (Figure 4) and used for the three-dimensional splat flow predictions.

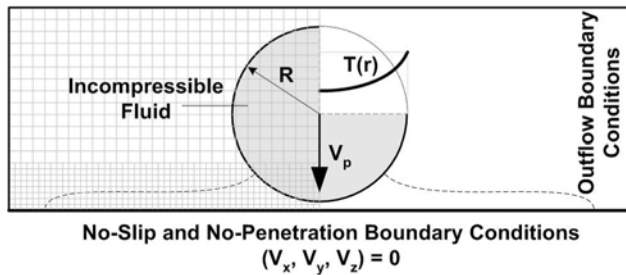


Figure 3: Boundary conditions, initial conditions and cross-section of a typical mesh used in Flow-3D<sup>®</sup>.

Splating of a 90  $\mu\text{m}$  diameter Nylon 11 droplet was predicted on both an ideally flat surface and on rough surfaces with average roughnesses ( $R_a$ ) of 1.48, 2.96 and 5.92  $\mu\text{m}$ . A roughen 3D surface was imported into Flow-3D<sup>®</sup> from an optical interferometry scan of an actual grit blasted steel surface (Figure 5b) with an average roughness  $R_a = 2.96 \mu\text{m}$ , as typically used for thermally sprayed coatings. A grit blasted surface was scanned by Zygo Corporation using NewView 6000 3D optical profiling system. The roughness of the imported surface was also numerically scaled to generate two additional surfaces with average roughness of 1.48 and 5.92  $\mu\text{m}$  for a parametric study.

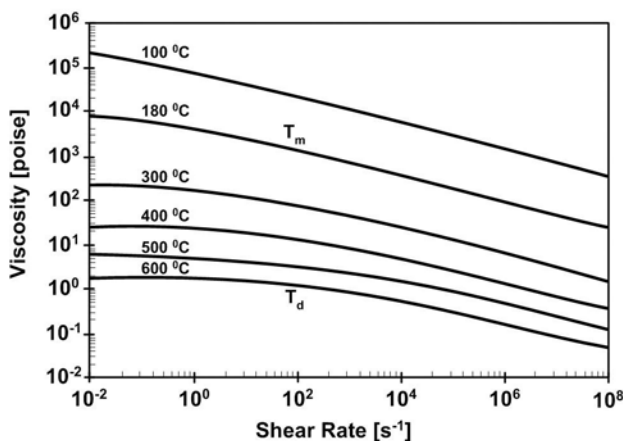


Figure 4: Shear rate and temperature dependent viscosity of Nylon 11 predicted using a Carreau model.

## Experiments

A semicrystalline Polyamide (Nylon 11) powder commercially available as Rilsan PA-11 French Natural ES D-60 (donated by Arkema) was used as the feedstock material in

this work. The as-received powder had a mean particle size of 60  $\mu\text{m}$  and corresponding particle size distribution of (-102, +26  $\mu\text{m}$ ). The melting and degradation temperatures of Nylon 11, as reported by the manufacturer, were in the range 182 - 191  $^{\circ}\text{C}$  and 357 - 557  $^{\circ}\text{C}$ , respectively.

Swipe or “splat” tests involving single high speed [ $> 0.7 \text{ m/s}$ ] spray passes across room temperature steel substrates at low powder feed rates ( $\sim 2 \text{ g/min}$ ) were used to observe the morphology of individual splats. The substrates used were 25 x 25 x 3 mm coupons of 4140 steel. The steel substrate was grit blasted using 125  $\mu\text{m}$  (120 mesh), 300  $\mu\text{m}$  (50 mesh) and 1500  $\mu\text{m}$  (12 mesh) alumina grit at an angle of 45 $^{\circ}$  with an air pressure of 0.55 MPa. The cross section of the grit blasted substrates was prepared using standard metallographic techniques: sectioning, mounting and polishing, and analyzed by optical microscopy using an Olympus PMG-3 optical metallograph.

Splat tests were carried out using the Stellite Coatings, Inc. Jet-Kote II<sup>®</sup> HVOF spray system using an  $\text{O}_2/\text{H}_2$  ratio of 0.0024/0.0039  $\text{m}^3/\text{s}$  (300/500 scfh) with a spray distance of 200 mm. Splat morphologies were analyzed using an FEI XL-30 field-emission Scanning Electron Microscope (SEM).

## Results and Discussion

### Experimental Results

The cross-sections of one polished and three grit blasted steel substrates used for the splat tests are shown in Figure 5. The morphologies of Nylon 11 splats deposited over these four surfaces during a single spray run are shown in Figure 6. Most of the larger splats ( $> \sim 100 \mu\text{m}$ ) observed on all four substrates exhibited a characteristic “fried-egg” shape with a large, nearly-hemispherical, core in the center of a thin disk. This observation was consistent with the previously reported [10] splat shapes deposited onto a flat glass slide substrate (Figure 2b), however, a preliminary observation, after SEM analysis of the multiple splat regions, indicated that the final splat diameter decreased as the substrate roughness increased. Statistical analysis and quantification of this observation is in progress.

Preliminary observations also indicated that an increase in general substrate roughness promoted splat instability, resulting in radial jetting and break-up, and producing more irregularly shaped splat shapes on rougher surfaces. Furthermore, it was observed that fingers on the periphery of the “fried egg” shaped splats solidified and settled on top of rough substrate asperities (Figure 7). This was believed to be due to the high speed squeezing flow of the leading edge of the splat leading rim over the top of the substrate asperities.

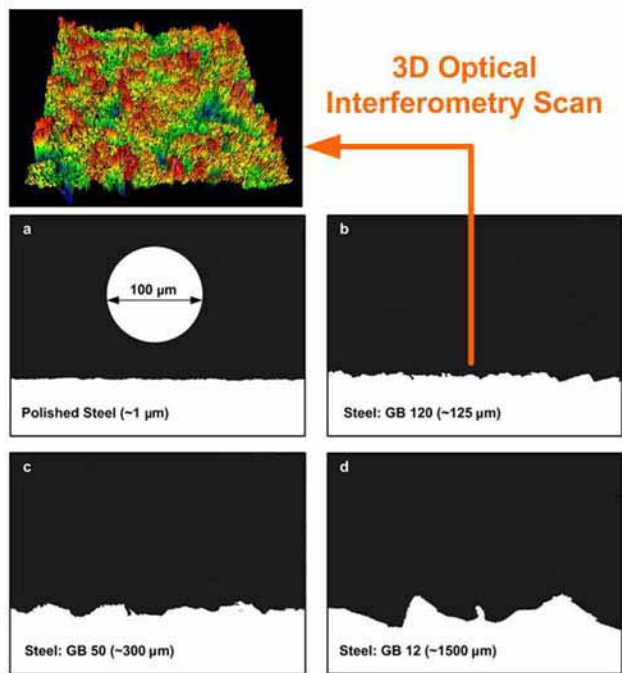


Figure 5: Cross section of four steel substrates: (a) polished with  $\sim 1 \mu\text{m}$  alumina suspension, (b) grit blasted with #120 grit, (c) grit blasted with #50 grit, (d) grit blasted with #12 grit. Top image shows optical interferometry scan of # 120 grit blasted surface.

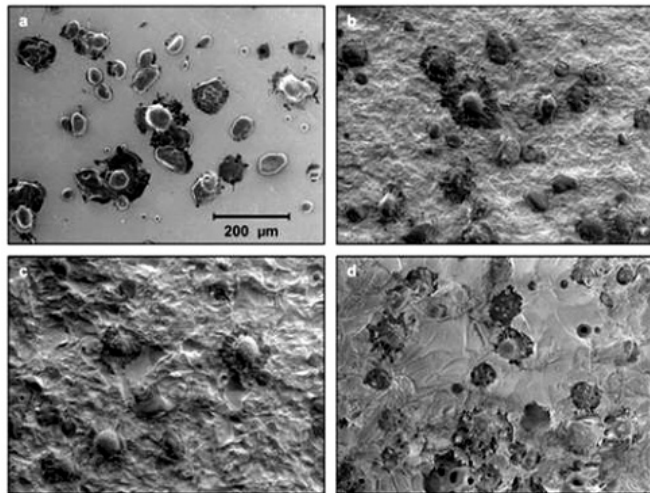


Figure 6: Nylon-11 splats deposited during a single run over steel substrates with roughnesses as per Figure 5.

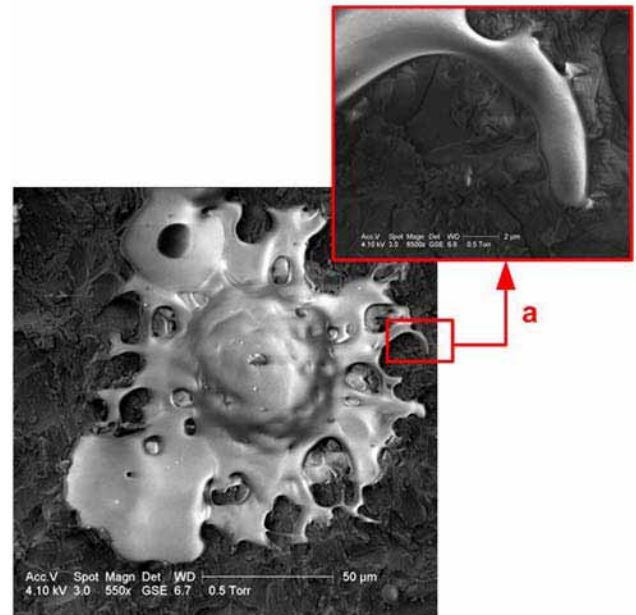


Figure 7: Nylon-11 splat on a grit blasted steel substrate, (a) close up of a peripheral splat finger.

### Modeling Predictions

Predicted three-dimensional cross-sections of spreading splats on four different substrate surfaces are shown in Figure 8. The predictions exhibited a good qualitative agreement with the experimentally observed splats shown in Figure 6 and 7. Larger splat spreading ratios ( $D_{\text{final}}/D_{\text{initial}}$ ) occurred on smoother surfaces, i.e. larger diameter splat were predicted on an ideally flat surface (Figure 8). Moreover, splat jetting/fingering was promoted as the substrate surface roughness increased, with the most prominent jetting occurring on the roughest surface, as indicated by the yellow and red splat fingers in Figure 8.

Cross-sections of the predicted three-dimensional  $90 \mu\text{m}$  diameter splat revealed a fully conformed interface between the center of the splat and the underlying substrate topography (Figure 8, detail A) while high speed radial jets spread over the substrate asperities, (Figure 8, detail B). This was believed to be due to the high stagnation pressure below and around the center of the splat including a flow mainly directed normal to the surface, promoting filling of the surface cavities. On the other hand, after impact the droplet developed a *leading edge* with a relative velocity higher than the original impact velocity (Figure 2a). The high velocity within the rim was the result of the squeezing flow between the relatively viscous particle core and the rigid substrate. This high shear rate flow led to low viscosity due to shear thinning, resulting in the very thin ( $2 - 5 \mu\text{m}$ ) splat rim. The low viscosity-high shear rate in the rim and interaction with the substrate roughness contributed to the formation of jets and fingers. These



predictions were in agreement with the experimentally observed radial finger morphology shown in Figure 7.

### Summary and Conclusions

A mathematical particle splatting model and experimentally captured splats on non-smooth surfaces have been studied in order to better understand how the geometrical irregularities of a generally roughened surface affect the final splat morphology. The morphology of the splats initially thermally sprayed onto a substrate surface play an important role in the integrity of the coating/substrate interface and the overall adhesive strength of the coating. This is because the primary bonding mechanism of thermally sprayed coatings is mechanical interlocking between the coating material and asperities on the roughened substrate.

Results, both experimental and numerical, indicated that the increase in magnitude of the mean substrate roughness promotes splat instability (jetting and/or satellite break-up) and formation of radial fingers. It was also observed that the

increase in general surface roughness may result in the lower spreading ratio ( $D_{\text{final}} / D_{\text{initial}}$ ) of thermally sprayed polymer particles.

The results also indicated that the center of a splat conformed well to the underlying substrate topography due to stagnation pressure and low shear rate flow directed steeply toward the surface encouraging the fluid to flow into surface cavities. On the other hand, a high speed leading edge of a splat resulted from the squeezing flow between the viscous particle core and the rigid substrate. The low viscosity-high shear rate within the rim and interaction with the substrate roughness contributed toward the formation of radial jets and fingers which flowed mainly parallel to the surface over the substrate asperities.

Statistical analysis of splats and further model development through the use of prototypical rough surfaces, e.g. steps and grooves are in progress.

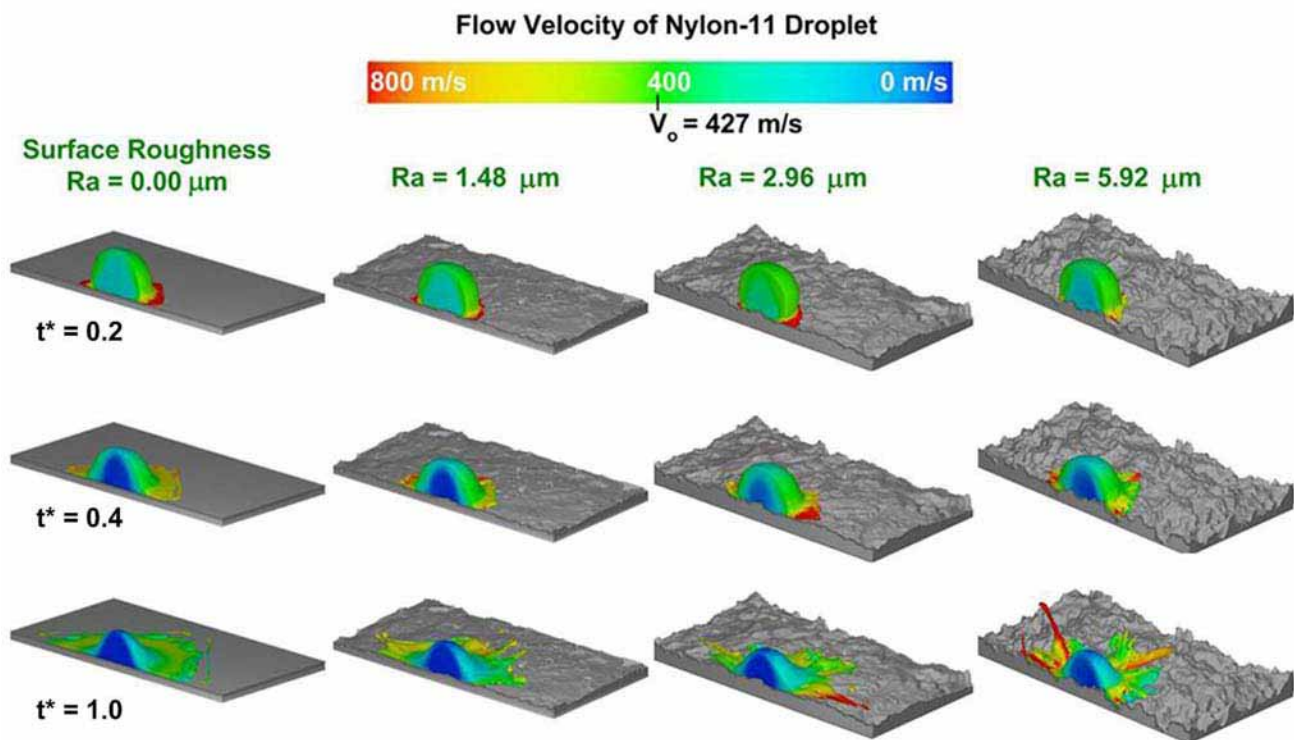


Figure 8: Cross-sections of predicted three-dimensional spreading splats for a 90  $\mu\text{m}$  diameter Nylon-11 particle on four different surface roughnesses (dimensionless time  $t^* = t/(D/v_o)$ ).

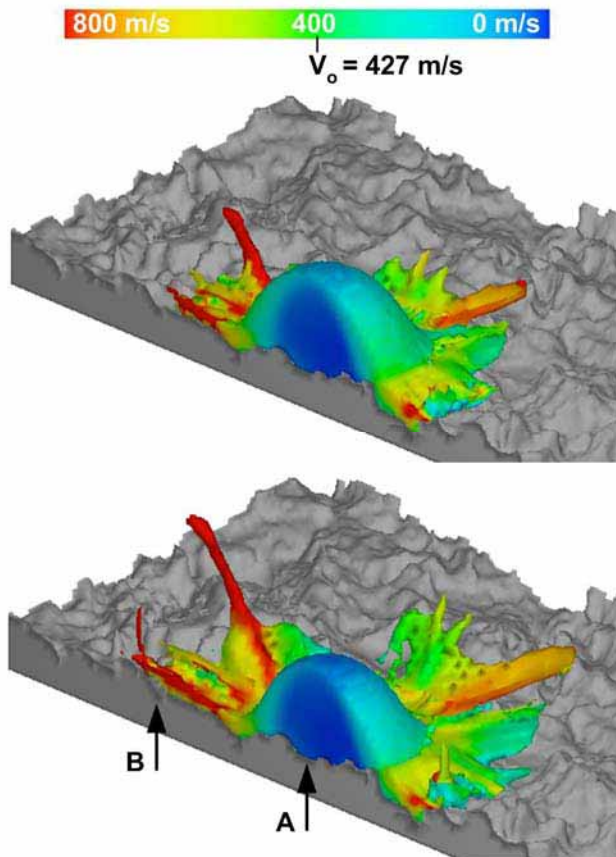


Figure 9: Predicted three-dimensional spreading splats for a  $90\ \mu\text{m}$  diameter Nylon-11 droplet.

#### Acknowledgments

The authors would like to thank the National Science Foundation for providing support for this research under collaborative grant number DMI 0209319. The views expressed in this paper do not necessarily reflect those of NSF. The authors also greatly appreciate the assistance and help of Mr. Dustin Doss. The assistance of Zygo Corp. with the surface roughness measurements reported here is also gratefully acknowledged.

#### References

1. Davis, J. R., (Ed.) et al, *Handbook of Thermal Spray Technology*, ASM International®, 1<sup>st</sup> Ed., Materials Park, OH, (2004).
2. Fauchais, P., Fukumoto, M., Vardelle, A. and Vardelle, M., Knowledge Concerning Splat Formation: An Invited Review, *Journal of Thermal Spray Technology*, 13 (3), pp. 337 - 360, (2004).
3. Liu, H., Lavernia, E. J. and Rangel, R. H., Modeling of Molten Droplet Impingement on a Non-flat Surface, *Acta Metall. Mater.*, 43(5), pp. 2053 – 2072, (1995).

4. Sobolev, V. V., Guilemany, J. M. and Martin, A. J., Influence of Surface Roughness on the Flattening of Powder Particles during Thermal Spraying, *Journal of Thermal Spray Technology* 5(2), pp. 207 – 214, (1996).
5. Patanker, N. A. and Chen, Y., Numerical Simulation of Droplet Shapes on Rough Surfaces, Proc. Int. Conference on Modeling and Simulations of Microsystems – MSM 2002, pp. 116 – 119, (2002)
6. Raessi, M., Mostaghimi, J. and Bussmann, M., “Droplet Impact during the Plasma Spray Coating Process-Effect of Surface Roughness on Splat Shapes,” Proc. 17<sup>th</sup> Int. Symposium on Plasma Chemistry – ISPC 17, Toronto, Canada, (2005)
7. Pasandideh-Fard, M., Chandra, S. and Mostaghimi, J., A Three-dimensional Model of Droplet Impact and Solidification, *Int. J. Heat and Mass Transfer*, 45, pp. 2229 - 2242, (2002).
8. Feng, Z. G., Domaszewski, M., Montavon, G. and Coddet, C., Finite Element Analysis of Effect of Substrate Surface Roughness on Liquid Droplet Impact and Flattening Process, *J. of Thermal Spray Technology*, 11(1), pp. 62-68, (2002).
9. Petrovicova, E., “Structure and Properties of Polymer Nanocomposite Coatings Applied by the HVOF Process,” Ph.D. Dissertation, Drexel University, (1999).
10. Ivosevic, M., Cairncross, R. A., Knight, R., Impact Modeling of Thermally Sprayed Polymer Particles, Proc. ITSC-2005 International Thermal Spray Conference, DVS/IIW/ASM-TSS, Basel, Switzerland, (2005).
11. Bao, Y., Gawne, D. T. and Zhang, T., The Effect of Feedstock Particle Size on the Heat transfer Rates and Properties of Thermally Sprayed Polymer Coatings, *Trans. I. M. F.*, 73(4), pp 119 – 124, (1998).
12. Ivosevic, M., Cairncross, R. A. and Knight, R., “Heating and Impact Modeling of HVOF Sprayed Polymer Particles,” Proc. 2004 International Thermal Spray Conference (ITSC-2004), DVS/IIW/ASM-TSS, Osaka, Japan, (2004).
13. Hirt, C. W. and Nichols, B. D., Volume of Fluid (VoF) Method for the Dynamics of Free Boundaries, *Journal of Computational Physics*, 39, pp. 201 - 225, (1981).